

Article

Combustion of Coal and Coal Slime in Steam-Air Environment and in Slurry Form

Vadim Dorokhov, Geniy Kuznetsov and Galina Nyashina *

Heat and Mass Transfer Simulation Laboratory, National Research Tomsk Polytechnic University, 30 Lenin Avenue, 634050 Tomsk, Russia

* Correspondence: gsn1@tpu.ru; Tel.: +7-(3822)-701-777 (ext. 3463)

Abstract: One of the ways to minimize anthropogenic emissions from coal combustion is to replace conventional schemes used for the introduction of coal dust into the furnaces of power plants through the injection of water-containing fuels. In this research, the three most promising schemes for fuel combustion were implemented: (i) the simultaneous introduction of coal particles and water droplets into the combustion chamber; (ii) steam injection into the fuel particle combustion zone; and (iii) the introduction of coal–water slurries into the furnace. Three methods of supplying water to the combustion zone were evaluated using the multi-criteria decision-making technique. Experimental research was conducted to record a range of process characteristics: the time of the gas-phase and heterogeneous ignition, the time of complete combustion, minimum ignition temperatures, maximum combustion temperatures, the completeness of the fuel burnout and the concentrations of the main gaseous emissions. It has been found that the most favorable scheme for coal particle combustion in water-steam environments is to produce fuel slurries. The cumulative indicator integrating the energy and environmental characteristics is 7–47% higher for slurries than for the other examined schemes for burning coal particles and slime.

Keywords: clean coal technologies; coal–water slurry; combustion; anthropogenic emission; steam; energy conservation



Citation: Dorokhov, V.; Kuznetsov, G.; Nyashina, G. Combustion of Coal and Coal Slime in Steam-Air Environment and in Slurry Form. *Energies* **2022**, *15*, 9591. <https://doi.org/10.3390/en15249591>

Academic Editor: Rajender Gupta

Received: 21 November 2022

Accepted: 13 December 2022

Published: 17 December 2022

Publisher's Note: MDPI stays neutral with regard to jurisdictional claims in published maps and institutional affiliations.



Copyright: © 2022 by the authors. Licensee MDPI, Basel, Switzerland. This article is an open access article distributed under the terms and conditions of the Creative Commons Attribution (CC BY) license (<https://creativecommons.org/licenses/by/4.0/>).

1. Introduction

At present, fossil fuel is used to meet 80% of the world's energy demands [1–3]. Coal combustion accounts for over 27% of the energy output [2,4], resulting in the emissions of the oxides of sulfur (up to 55% of all the world's SO₂) and nitrogen (up to 25%), carbon dioxide (up to 45%) and fine ash particles (PM_x) (up to 20%) [5,6]. A high degree of the hazards caused by these substances for human health and their impact on the environment were analyzed in [7–10]. Sulfur oxides (SO_x) entering the atmosphere may cover hundreds of kilometers and, after interacting with steam-form H₂SO₄, can be precipitated as acid rains. People living in areas with heavy sulfur oxide emissions often develop symptoms of respiratory diseases [7]. Nitrogen oxides, being the second most toxic combustion product of pulverized coal fuel, turn to HNO₃ in the air and are the most common component of acid rains [7]. The vapors of these acids enter the respiratory system aggravating respiratory diseases [11]. That is why the environmental aspects of coal combustion in power plants become a pressing task. One of the ways to deal with the environmental problems caused by a high level of anthropogenic emissions produced by the combustion of traditional coal is to replace it with coal–water slurries with and without petrochemicals (CWSP and CWS) [12–14]. The anthropogenic emissions from the combustion of water-containing fuels based on coal and coal-processing waste are lower than from pulverized fuel [15–17]. Significantly, such slurry fuels feature comparable or even better energy characteristics than conventional boiler fuel types [13–15,18,19]. There are research findings [5,20,21] in which water, in the form of steam, was supplied to the fuel combustion zone and

improved the efficiency of heat generation and reduced the emissions of NO_x and CO in the flue gas composition. Another combustion scheme involves the simultaneous introduction of solid fuel particles and water droplets into the combustion chamber by injection through nozzles and burner units [22]. Such methods of applying water and steam in coal combustion systems have several advantages. Unlike slurries, they do not require any significant upgrades to the fuel-feeding systems at power plants. Using steam as the combustion atmosphere component makes it possible to increase the combustion temperature and the completeness of fuel burnout, as well as to reduce the ignition duration and temperature [23–25].

Steam is crucial for controlling the reaction rates in the combustion chamber. Its role changes when the process parameters (in particular, the temperature, pressure and concentration of steam) are varied. Gil et al. [26], for instance, studied the effect of steam in the reaction zone on the combustion behavior of pulverized coal. In this study, 10 and 20 vol% steam was introduced into the combustion chamber. The initial, final and maximum temperatures of combustion, the rates of mass loss and the reactivity index of coal were recorded. Adding steam was found to reduce the combustion temperature and burnout time, while increasing the burnout rate [26]. Wang et al. [20] investigated the effect of H_2O on the thermal decomposition characteristics of pulverized fuel using a TGA analyzer. The burnout time and rates, as well as the mass fractions of the combustible residue of three kinds of coal were recorded with different concentrations of steam and oxygen. It was shown that with an increase in the steam concentration (from 10 to 30%), the coal burnout time decreased. A temperature rise magnified the positive effect of steam on combustion characteristics. For example, when steam was used at a temperature of 700 °C, the burnout rate increased by 5%; at 1000 °C, the reaction rates grew by 15–25% [20]. This result is conditioned by the active gasification of coal with steam. This process increased the porosity of coal particles and the rate of oxygen diffusion into the inner coal structure [21]. The impact of steam supplied during coal pyrolysis was investigated in [27]. In the experiments, steam was mixed with argon. The concentration of steam in the mixture ranged from 2 to 67%. An increase in the steam led to higher CO_2 and lower CO concentrations in the producer gas. With 2% steam, the proportion of CO and CO_2 in the gas was 72.4% and 26.8%. With steam content increased to 67%, the proportion of CO and CO_2 was 34.4% and 63.8%, respectively. This is accounted for by the fact that an increase in the steam concentration led to more active and lengthy gas-phase combustion, contributing to the CO_2 yield [27]. The findings for the effect of atmosphere in a fixed-bed reactor on NO_x emissions from the pyrolysis of bituminous coal are presented in [28]. The NO_x concentration from the pyrolysis in the air atmosphere was $1.2 \text{ g}_{\text{NO}_x} / \text{g}_{\text{fuel}}$. During pyrolysis in a steam-air environment, the concentration of nitrogen oxides decreased by more than 1.5 times. Lei et al. [23] present the research findings for the ignition and combustion behavior of bituminous coal pellets and sewage slime. The experiments were conducted in three different combustion atmospheres: O_2/N_2 , O_2/CO_2 and $\text{O}_2/\text{CO}_2/\text{H}_2\text{O}$. It was established [23] that replacing 10–30% CO_2 with steam reduced the fuel ignition delay times by 10–40%. This is conditioned by the high volumetric heat capacity of steam compared to CO_2 . Similar results were obtained in [24]. It was established, in particular, that using steam reduced the burnout duration and increased the maximum combustion temperature of a fuel particle due to the higher intensity of thermal decomposition. The characteristics of bituminous and brown coal particle ignition in the oxy-steam combustion atmosphere were examined in [29]. The steam content varied in the range of 0–40%. It was demonstrated in the experiments that with 10% steam, the threshold ignition temperatures of fuel particles were minimal. For bituminous coal, the ignition temperature decreased by 16 °C, and for brown coal by 19 °C. A further increase in the steam amount led to a higher ignition temperature. Using steam in the combustion atmosphere was also found to affect the formation of CO and NO. For bituminous coal, the concentrations of nitrogen oxides decreased, and CO increased with a rise in the steam content. In turn, with brown coal, an increase in the steam content increased the CO and NO concentrations.

2. Motivation and Aim of the Research

The analysis of the research findings cited above revealed that a steam-air environment has a significant effect on the combustion characteristics of coal fuels. Yet there are different ways of supplying steam to the fuel combustion zone. It is reasonable to perform a comparative analysis of the effect of the method used to create a steam-air environment on the conditions of solid fuel particle combustion. There are currently no studies comparing the gas-phase (τ_{d1}) and heterogeneous (τ_{d2}) ignition delay times, combustion duration (τ_b), maximum (T_d^{\max}) and minimum (T_g^{\min}) combustion temperatures, the completeness of burnout and the concentrations of the main anthropogenic emissions (CO_2 , NO , SO_2) when introducing steam, water droplets or a coal–water slurry into the furnace environment. At present, there are no data on the effect of the steam-air environment on the combustion characteristics of coal-processing waste and slurries based on it. Thus, this research aims to determine experimentally the effect of the method of supplying water to the combustion chamber on the characteristics of coal fuel combustion. Three methods of supplying water (water in the slurry composition, the parallel introduction of water and coal component, and steam-air supply) to the combustion zone were evaluated using the multi-criteria decision-making (MCDM) technique.

3. Materials, Setup and Experimental Methodology

The coal components were coking bituminous coal from the Berezovskoe deposit (Kemerovo region, Russia) and coal slime was derived from the processing of coal of the same rank. Coal components were first ground in a rotor mill and riddled to obtain a fine powder with a particle size of no more than 100 μm . This pulverized powder was later used to produce slurries.

Figure 1 presents the layout of the setup used to determine the flue gas composition when varying the method of introducing water and the coal component into the combustion chamber. The fuels under study were burned in an electrical tube furnace R 50/250/13 (internal diameter of the ceramic tube 0.04 m, 0.45 m long; temperature range 20–1200 °C; the temperature is controlled by a signal of the built-in type S thermocouple) (Nabertherm GmbH, Lilienthal, Germany). To analyze the gas composition, a Test 1 gas analyzer (Bonaire-VT, Novosibirsk, Russia) was used. It included electrochemical sensors for O_2 (measuring range 0–25%, absolute error $\pm 0.2\%$), CO (measuring range 0–40,000 ppm, relative error $\pm 5\%$), SO_2 (measuring range 0–1000 ppm, relative error $\pm 5\%$), NO (measuring range 0–2000 ppm, relative error $\pm 5\%$), NO_2 (measuring range 0–500 ppm, relative error $\pm 7\%$), H_2S (measuring range 0–500 ppm, relative error $\pm 5\%$) and HCl (measuring range 0–2000 ppm, relative error $\pm 5\%$). The gas analyzer was additionally fitted with optical sensors for CO_2 (measuring range 0–30%, percentage error $\pm 2\%$), CH_4 (measuring range 0–30%, percentage error $\pm 5\%$) and CO (measuring range 0–30%, percentage error $\pm 5\%$) and a polarographic sensor for H_2 (measuring range 0–5%, absolute error $\pm 5\%$). The flow rate of flue gases into the gas analyzer (pump flow) was 0.6 l/min. Moreover, the device included a modular probe, a moisture collector and a filtration system to dry and clean the gas sample. To feed the fuel into the combustion chamber, a coordination mechanism automatically moved the fuel sample into a hollow heating tube in the furnace at 0.2 m/s. This speed was chosen to hold the sample steady in the combustion chamber. A coordination mechanism controlled by a computer was used. Test 1 software was installed on it. This was used for the real-time tracking of changing anthropogenic gas concentrations during combustion. In the experiments, the required temperature in the working zone of the combustion chamber was set on the control panel. It ranged from 700 to 900 °C. These temperatures ensured that all the typical ignition and combustion stages with the active release of gaseous substances took place [30–32]. The threshold temperature (900 °C) corresponded to the maximum achievable value that provided adequate operation of the main setup elements (muffle furnace and gas analyzer) without damage to their internal elements (the ceramic tube of the furnace and the electrochemical sensors of the gas

analyzer) as a result of the high temperatures. After the combustion chamber was heated to the given temperature, the fuel was fed to the combustion chamber using the manipulator.

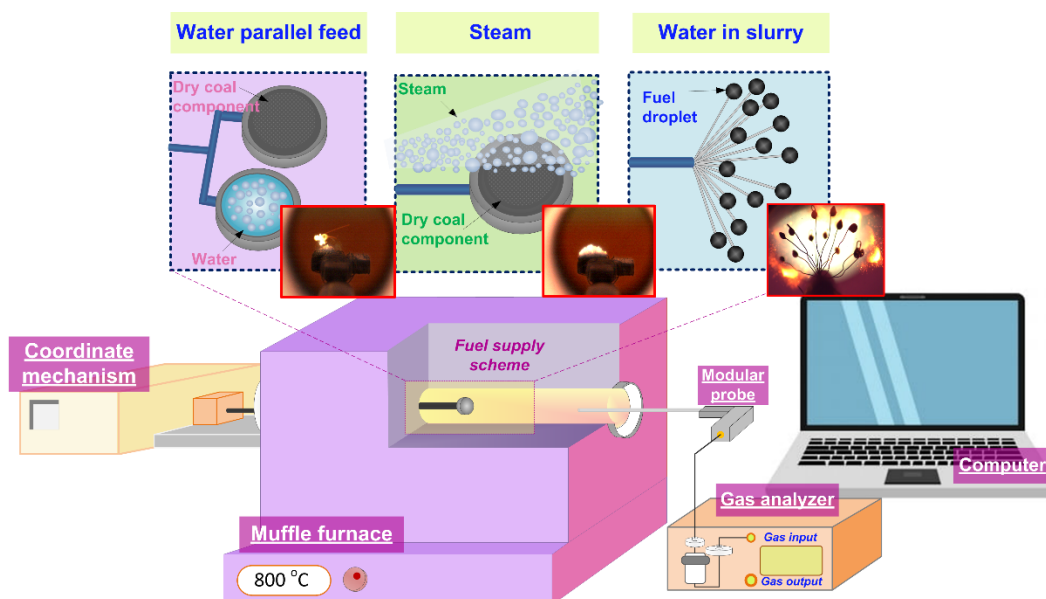


Figure 1. Experimental setup.

To implement the different methods of fuel introduction, several types of holders were used (the details in Figure 1). The simultaneous introduction of the water and the coal component was implemented on horizontal substrates. The dry coal component was fed as a thin layer evenly spread on the holder surface. Fine coal dust with an average particle size of 100 μm was used. The slurry was fed onto a holder made in the form of grouped thin rods on which droplets were suspended. For each option, the fuel mass was kept constant at 0.2 g (consequently, the coal component mass was 0.1 g, the same as the mass of water/steam). Thus, the number of slurry droplets and their mass were chosen so that the total mass of the fuel to be burned in the furnace was equal. A steam generator was employed to create steam. Steam was injected through the opening that was used to introduce the fuel into the furnace. After the fuel was in the furnace, the opening was sealed with a thick layer of thermal insulation material. On the opposite side, the modular probe of the gas analyzer was inserted into a similar-sized opening. The latter was sealed with the same material. Over the course of the ignition and combustion, flue gases went through the modular probe to the gas analyzer casing (passing through the drying and filtration stages), where the concentrations of the gas mixture components were measured. After the end of each experiment, the gas channels and the muffle furnace space were cleared with fresh air to remove the remains of the sample. Five to ten experiments were conducted in one series. After that, the errors were estimated. The time-averaged concentrations of gases were determined using the trapezoidal rule. A detailed description of this method was given in [33].

The ignition and combustion characteristics were recorded in the experiments by a Phantom Miro C110 high-speed video camera (Vision Research Inc, Wayne, NJ, USA), the rate of recording was 1000 frames per second at a resolution of 800×600 pixels. This equipment was installed in place of the gas analyzer. When processing the video recordings, the following combustion characteristics were determined: gas-phase and heterogeneous ignition delay times, and the duration of the fuel combustion. Tema Automotive Video software (Image Systems AB, Linköping, Sweden) was used to analyze the video recordings of the experiments. The ignition delay time was the interval from the moment when heating started up until the moment of ignition, characterized by a flame. The ignition of solid organic fuel is generally subdivided into two stages: gas-phase and heterogeneous ignition.

In this study, we also singled out these stages. The point of gas-phase ignition was identified visually by a flash of combustible gases around the fuel sample. The heterogeneous ignition of the solid residue was determined using a video recording and software to track the variation in the luminosity of the burning fuel surface. Thermal imaging Testo 885-2 (Testo SE and Co. KGaA, Lenzkirch, Germany) (measurement range 0–1200 °C, image resolution 640 × 680 pixels) was employed to determine the maximum combustion temperatures of the solid coke residue of the fuel. The minimum temperature of the fuel ignition T_{gmin} (i.e., the temperature above which stable combustion occurs) was recorded using a K-type thermocouple (temperature range 0–1100 °C, systematic error ± 3 °C, response time no more than 10 s), built into the muffle furnace. All ignition and combustion characteristics were determined from 5–10 repeat measurements, avoiding gross errors.

4. Results and Discussion

4.1. Combustion Stages and Mode

The analysis of the video recordings obtained revealed that the combustion of the fuels under study is characterized by the following stages: the drying and pyrolysis of the fuel, the gas-phase combustion of the mixture of the products of thermal decomposition of the solid component and the evaporation of the liquid combustible component, heterogeneous combustion of the coke residue. Figure 2 presents the video frames obtained when exposing the fuels based on coal slime to radiant heating at a combustion chamber temperature of 900 °C. Supplementary Material presents a typical video frame of the corresponding process. At the fuel drying and pyrolysis stage, there was an extensive release of volatiles accumulating in the close vicinity of the fuel particle surface. When the ignition temperature was achieved, the resulting gas mixture ignited and burned out. During this process, additional thermal energy was released and transferred to the fuel sample. In the final stage, the combustion of the carbonaceous residue occurred, which completed the thermal decomposition of the deep fuel layers. Typical frames (Figure 2) show that the gas-phase combustion of the slurry fuel is different from the other two options (with the parallel introduction of components and combustion in the steam-air environment). The gas-phase combustion of the slurry fuel droplets was characterized by a smaller cloud of reacting gases in the space around the fuel sample, whereas with a parallel (simultaneous) introduction of the components (water and coal) and water supplied as steam, the area of the jet of flame occupied a much larger volume in the combustion chamber. There are several reasons for that. First, a slurry droplet, whose size is comparable to a coal particle and a fine coal sample, contains a much smaller combustible part (its major share belongs to an inert component, water) and, consequently, fewer thermal decomposition products. Second, the release of water vapors and thermal decomposition products proceeds from the same droplet surface, taking the porous channels in the structure into account. This somewhat reduces the concentration of combustible gases around the droplet. Third, the thin near-surface layer of the slurry droplet becomes drier with the gas-phase combustion becoming more extensive. A limited amount of thermal decomposition products remains in this near-surface layer. Therefore, the size of the reacting gas-phase cloud in the vicinity of the slurry droplet is small.

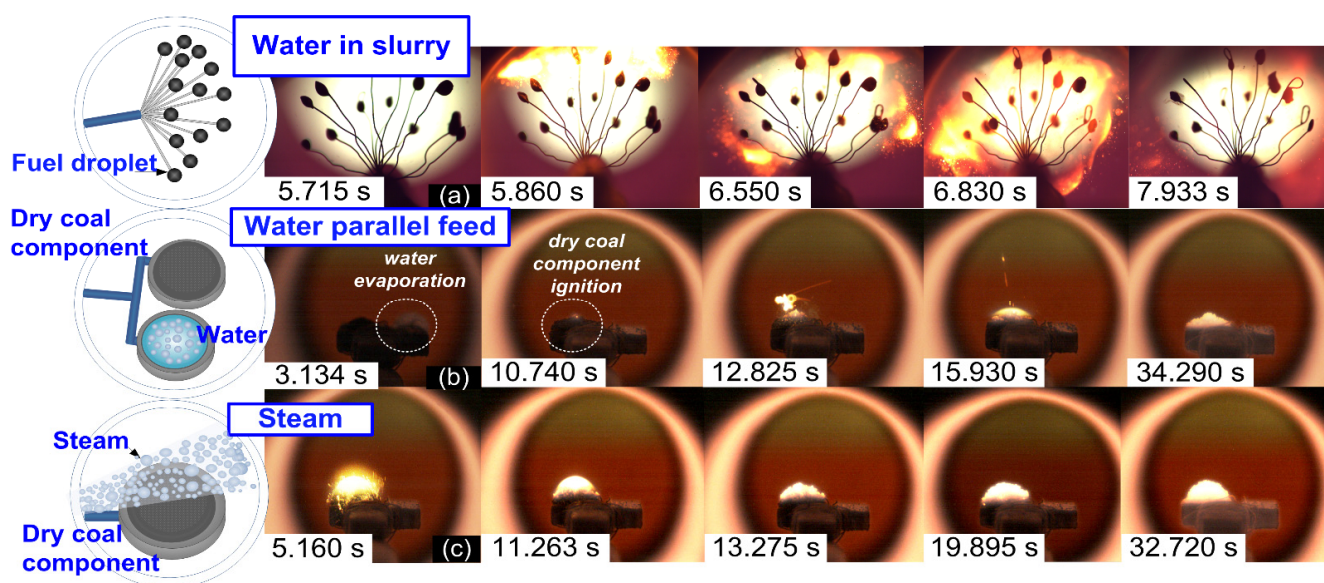


Figure 2. Video frames demonstrating the combustion of fuels based on coal slime at a combustion chamber temperature of 900 °C ((a)—water in the slurry composition; (b)—parallel introduction of components; (c)—water supplied as steam).

4.2. Ignition Characteristics

Figure 3 presents the curves for the gas-phase ignition delay time of the fuels under study versus the temperature in the combustion chamber. The highest ignition delay times were recorded when water was supplied in the form of droplets located in the close vicinity of the coal particles/slime piled on the substrate. This result is accounted for by the fact that quite a substantial amount of energy was spent on the heating and evaporation of liquid and the subsequent heating of vapors (whose specific heat capacity is twice as high as that of air). Therefore, the ignition delay in this method of supplying water to the combustion chamber becomes longer. Unlike in the case of a steam flow, the introduction of liquid droplets required extra energy for their heating and evaporation. When solid fuel particles were fed to the combustion chamber filled with steam, the ignition delay times were the lowest. Compared with the combustion of coal and slime in the air, the gas-phase ignition delay times decreased by 27–50% and 25–59%, respectively. This result illustrates that the high heat capacity and optical properties (absorption, transmission, reflection and the refraction of radiation) of the steam have a positive effect on the heating, pyrolysis and gas-phase ignition of volatiles. The energy accumulated in the thin water layer in the near-surface layer of the slurry droplet contributes to the quite significant local heating of the solid coal particles [34]. The latter are pyrolyzed, and a gas–vapor mixture is formed in the thin near-surface layer close to the coal particles and the slurry droplet. This mixture has a high concentration of combustible gases and a rather high temperature at which gas-phase combustion occurs. This process increases the fuel surface temperature, enhances the volatile release and heats the solid framework that later ignites. Heterogeneous combustion takes place. Steam immensely absorbs radiation and accumulates the heat around the reacting fuel. This effect is crucial in this system. Steam injection into the combustion chamber somewhat reduces the gas medium temperature in the vicinity of fuel particles, but due to radiation absorption, the temperature quite quickly returns to the original values and then rises. When water slurry droplets are used, the fuel actively reacts at the initial stage in the thin near-surface layer. The video frames of the experiments revealed that the near-surface layers of the water slurry droplet are extensively heated when they are introduced into the combustion chamber; the gas-phase combustion begins, followed by heterogeneous combustion.

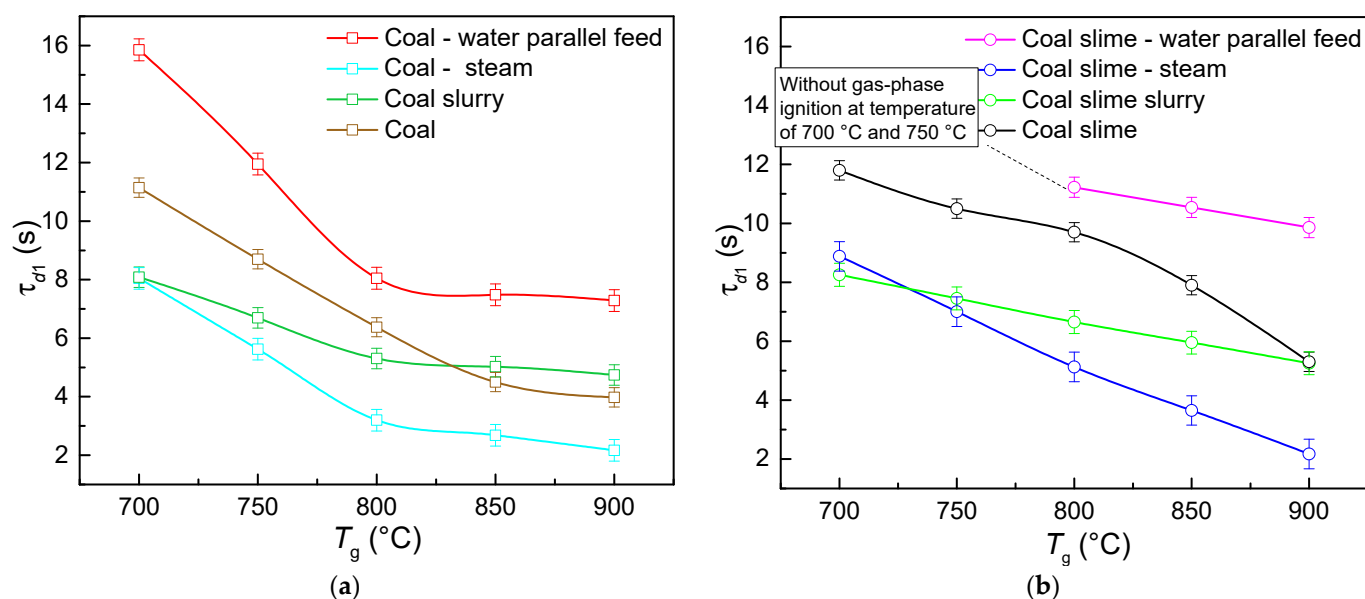


Figure 3. Gas-phase ignition delay times of fuels based on bituminous coal (a) and coal slime (b) when varying the method of introducing the components and temperature in the combustion chamber.

The conducted experiments showed that when water droplets were fed in simultaneously alongside a pile of coal slime particles, the gas-phase combustion stage in the temperature range of 700–800 °C was not very pronounced. The gas-phase combustion became more active with the increase in the temperature in the furnace to 800 °C (Figure 3b). Extensive gas-phase combustion was not recorded even at lower temperatures in the chamber. In the thin near-surface layer, weak luminance was recorded, indicating the gas-phase combustion of the products of thermal decomposition of the carbon-containing solid particles. The recording of the conditions of the marked gas-phase combustion of pyrolysis products at relatively low temperatures in the chamber was complicated by extensive vaporization. The steam reduced the temperature of the gas-vapor mixture. Another important factor was the limited content of volatiles in coal slime (Table 1).

Table 1. Proximate and ultimate analysis of components used in the experiments.

Component	W ^a , %	A ^d , %	V ^{daf} , %	Q ^{a_{s,v}} , MJ/kg	C ^{daf} , %	H ^{daf} , %	N ^{daf} , %	S _t ^d , %	O ^{daf} , %
Coal	2.05	14.65	27.03	29.76	79.79	4.486	1.84	0.868	12.70
Coal slime	43.5	26.46	23.08	24.83	87.20	5.090	2.05	1.022	4.46

Here W^a is moisture content; A^d, S_t^d are, respectively, ash and sulfur content on a dry basis; V^{daf}, C^{daf}, H^{daf}, N^{daf}, O^{daf} are, respectively, volatile, carbon, hydrogen, nitrogen and oxygen content to a dry ash-free state; Q^{a_{s,v}} is higher heat value.

At high temperatures in the chamber, e.g., at 800 °C, the flame combustion of a slime layer was sustainably recorded, yet it took 13–46% more time for the gas-vapor mixture to achieve it than in the combustion of coal slime of the same mass in the air (Figure 3b).

Introducing slurry fuel droplets into the combustion chamber was characterized by the average ignition delay times of the fuel samples under study. This is explained by the fact that the gas-phase ignition of the slurry fuel is only possible after the moisture preventing the release of volatiles from the fuel surface evaporates from the near-surface layer. In turn, using steam enhanced the fuel ignition without any extra heat lost upon evaporation.

It was also established that with all the fuel-feeding schemes under consideration, using bituminous coal leads to a lower ignition delay time than when coal slime is used. This is accounted for by the fact that bituminous coal contains more volatiles (Table 1)

whose gas-phase combustion contributes to a significant increase in the temperature of the coke residue and thus in the rates of its heterogeneous combustion.

To justify the comparison of the integral characteristics of the ignition and combustion of a group of slurry droplets and a thin layer of coal particles spread on a substrate, additional experiments were conducted. The results are shown in Figure 4. When a slurry droplet, a coal powder pile and a single large coal particle, all of an identical size, were ignited, the gas-phase ignition of the slurry occurred sooner than that of the coal samples. The solid coal particle ignited later than the other fuel samples. This is because the particle size of coal powder in a pile and of the slurry was smaller than that of the single coal particle. The gas-phase reaction of the slurry droplet and coal pile with solid particles of the same size was characterized by almost identical ignition delay times. This result demonstrates the decisive role of the size of solid particles in the composition of the pile and slurry. The finer the solid particles, the weaker the effect of water on the time lag in the heating of the near-surface layer of slurry droplets. Their heating time until they ignite is the same as that of the samples of identical particles that were not additionally wetted. These specific aspects have a significant effect on the subsequent heterogeneous reaction of the coke residue.

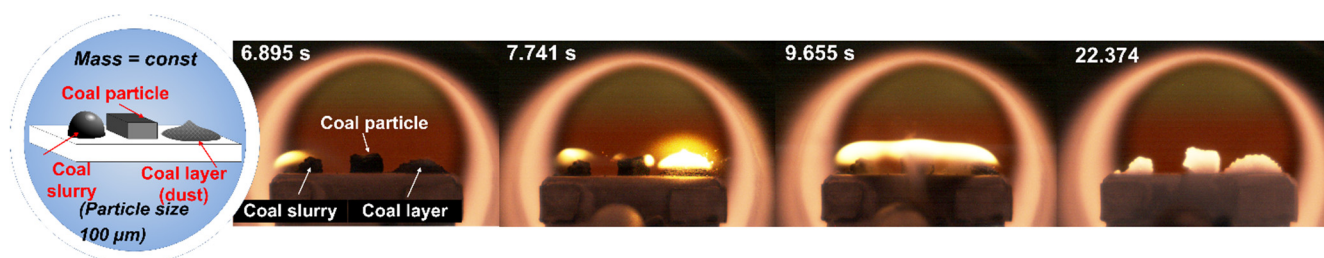


Figure 4. Video frame of the fuel combustion under identical conditions of feeding the fuel to the combustion chamber at 800 °C.

Figure 5a presents the experimentally obtained curves of the heterogeneous ignition delay times of the fuels based on coal versus the temperature in the furnace. Bituminous coal dust reacting in the air medium has the highest delay times of heterogeneous ignition. Creating a steam-air environment when introducing separate water droplets on the substrate or when supplying steam makes it possible to reduce the heterogeneous ignition delay times of the coke residue of coal by 14–33% and 46–52%, respectively. Although the gas-phase ignition of coal (Figure 3a) occurred more slowly when it was in parallel with the water supply, the heterogeneous ignition was recorded sooner than for the reactions of coal particles without water droplets around them. The temperature conductivity of water vapors is lower than that of the air. Consequently, the heat released from the combustion of volatiles in the presence of water vapors spreads more slowly throughout the combustion chamber volume and is concentrated on the surface of coal particles. The coke residue ignition proceeded faster. Similar effects were observed in [21]. The effect of the steam environment on the characteristics of pulverized coal combustion in the O_2/CO_2 atmosphere was explored. The presence of water vapors was shown to lead to faster burnout and increase the overall reactivity of coal. The diffusion rate of O_2 in the atmosphere of steam is claimed [21] to be much higher, which is responsible for the reaction intensification.

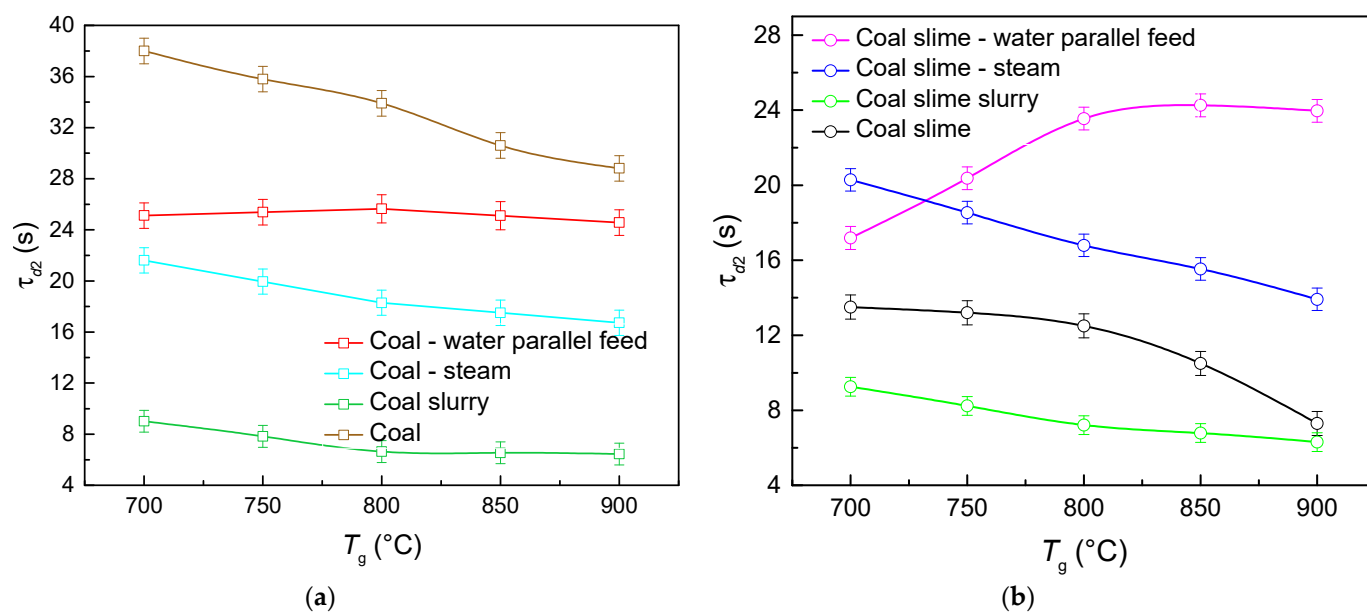


Figure 5. Heterogeneous ignition delay times of fuels based on bituminous coal (a) and coal slime (b) when varying the method of introducing the components and temperature into the combustion chamber.

In the case of coal slime (Figure 5b), the specified effect of the rapid reaction of the near-surface layer of droplets led to the agglomeration of particles on the fuel surface and the formation of a coke envelope that slowed down the release of volatiles and their mixing with oxygen. Thus, the gas-phase combustion rates slightly decreased. This increased the heterogeneous ignition delay times of coal slime when it was heated in the steam environment (as compared with the combustion of coal in a steam environment). The heterogeneous ignition of coal slime in the air started 21–69% faster. When a coal slime sample was fed in simultaneously with water droplets, there was an increase in the heterogeneous ignition delay time with a temperature rise from 700 to 800 °C. This is caused by the fact that, at combustion chamber temperatures lower than 800 °C, no extensive gas-phase combustion of pyrolysis products or evaporation of components of this fuel was recorded. Irrespective of the type of the coal component, the combustion of solid fuel particles in the slurry droplet composition was characterized by the shortest gas-phase combustion (the process developed actively), which, in turn, led to low heterogeneous ignition delay times. The transition from gas-phase combustion to heterogeneous combustion occurred faster due to the heating of the thin near-surface layer. The heterogeneous ignition delay times of slurry droplets were 1.5–4 times lower than those of the other combustion schemes under study.

Figure 6 illustrates the lowest ignition temperatures of the fuels, determined experimentally for the combustion schemes under consideration. T_g^{\min} is the minimum temperature in the furnace at which the steady heterogeneous combustion of solid fuel particles occurs. The highest T_g^{\min} was recorded for the samples of coal and slime reacting in the air. The ignition of coal components in the steam-air environment, on the contrary, occurred at lower temperatures. Thus, T_g^{\min} for the coal–water suspension decreased by 16.7% in comparison with the dry coal combustion. The lowest ignition temperature was recorded in the experiments with a mixture of coal slime with water in a slurry composition. This result is likely to be conditioned by the specific aspects of liquid evaporation from the surface of the slurry fuel droplets. The water in the composition of the slurry based on coal slime evaporated faster than in the slurry based on bituminous coal due to the higher density and viscosity affected by the flocculants used for coal preparation. An increase in the concentration of vapors in the close vicinity of the sample facilitated its heating due

to radiant heat exchange. Therefore, to reduce the ignition temperature of coal fuels, it is advisable to use a water-steam-saturated atmosphere.

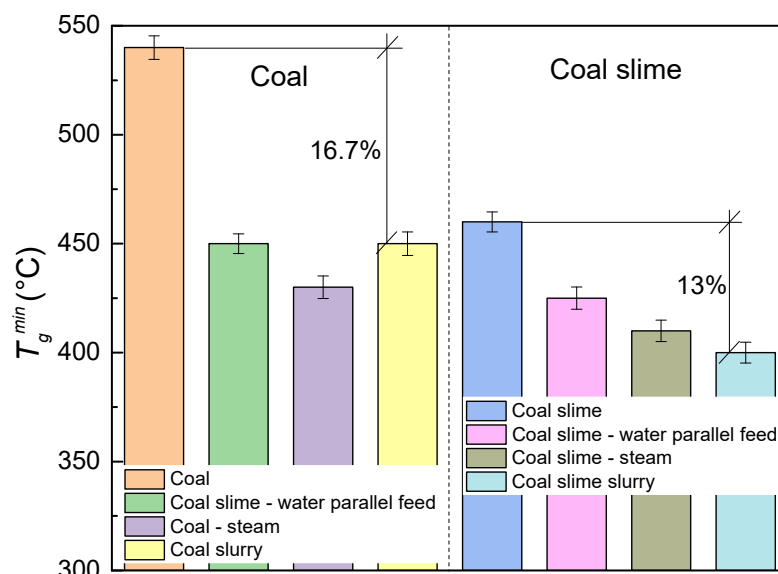


Figure 6. Minimum ignition temperatures of fuels based on bituminous coal and coal slime when varying the method of introducing the components into the combustion chamber.

4.3. Combustion Characteristics

Figure 7 presents the curves of the maximum combustion temperatures of the coke residue, obtained in the conducted experiments when varying the temperature in the combustion chamber. The recorded values of this parameter corresponded to the range of 875–1112 °C. The lowest maximum combustion temperature within the range under study is typical of the fuel slurry based on coal slime. This result might be related to the fact that combustion was more uniform when a slurry was used. In turn, with the simultaneous introduction of the components and the steam-air atmosphere in the combustion chamber, the temperatures in the fuel combustion zone increased and became comparable with those of the fuels reacting in the air medium. This is explained by the fact that rapid vaporization increased the diffusion rate of oxygen in the combustion zone and, thus, the rate of the interaction of carbon with vapor:



This interaction results in additional combustible gases. Their interaction with oxygen releases extra thermal energy, thus increasing the temperature in the reaction zone. A similar conclusion was drawn in [21]. It was established that during the combustion of three types of coals in the atmosphere with steam, the maximum temperatures of the combustion of samples increased by 5–10 °C. This result is explained by a higher rate of oxygen diffusion to the coal particles in the presence of water vapors. Moreover, the research showed that the maximum combustion rates and average mass-loss rates during the combustion of coal were significantly higher in the atmosphere with water vapors than in the N₂ atmosphere. However, despite the differences, the discrepancy between the maximum combustion temperatures in this research and those in [21] did not exceed 5%. This is conditioned by the fact that the main fuel component was the same (coal and coal slime). Its characteristics determine the maximum temperature of the heterogeneous combustion of carbon to a greater degree than the external gas-vapor medium does.

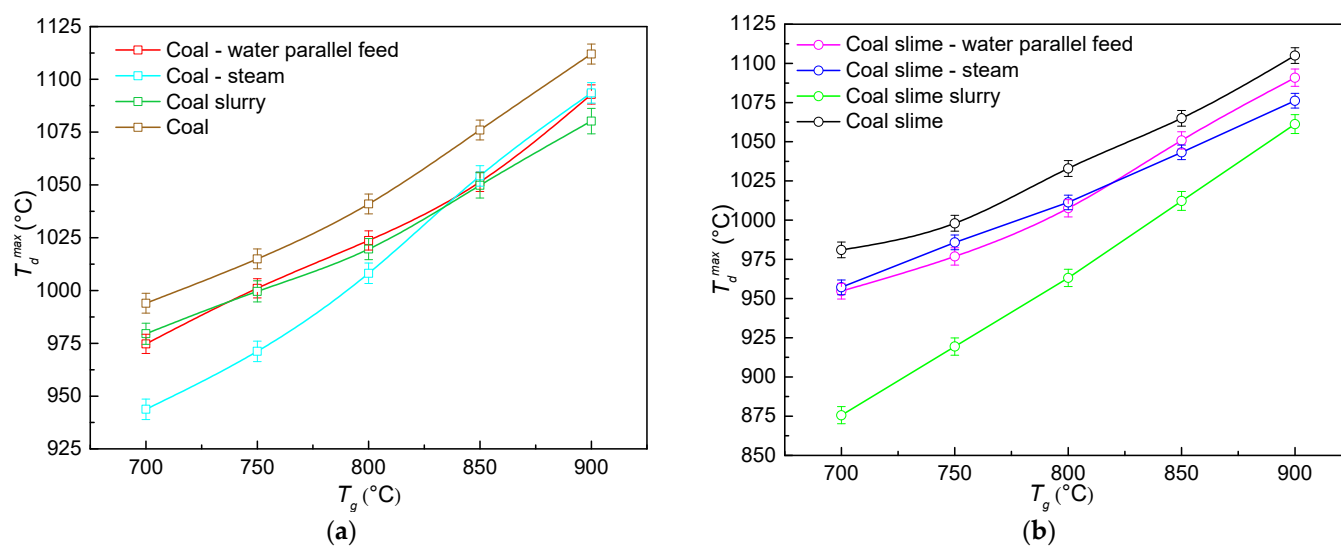


Figure 7. Maximum combustion temperatures of fuels based on bituminous coal (a) and coal slime (b) when varying the method of introducing the components and initial temperature in the combustion chamber.

The curves for the duration of the fuel combustion versus the temperature in the combustion chamber are presented in Figure 8. The obtained curves look significantly different for the three schemes of solid fuel combustion under the conditions of increased moisture in the furnace chamber. In the case of the parallel introduction of water droplets and solid fuel particles, the combustion duration of coal components increased with a temperature rise. This trend indicates that at lower temperatures, the combustion stopped before all the combustible parts of the fuel reacted. Substantial energy was spent on the evaporation of water droplets located near the solid fuel particles on the substrate. In addition, the specific heat capacity of the resulting water vapors is higher than that of the air. Therefore, a considerable amount of energy is required to heat them. Thus, a certain amount of energy was removed from the surface of the fuel, and it stopped burning faster in the areas of low temperatures. In this case, the fullest involvement of the combustible mass in the burnout is only possible by increasing the amount of heat supplied to the fuel sample.

In the case of combustion in a water-steam-saturated atmosphere, the duration of the fuel combustion decreased as the temperature in the muffle furnace went up. The supply of generated steam increased the reactivity of the fuel and promoted its more complete burnout compared to the simultaneous introduction of components [21].

The lowest combustion time was typical of slurry fuel droplets based on coal slime and bituminous coal. This effect is conditioned by the fact that the burned fuel mass is separated into a group of small droplets, which provided a free supply of oxygen to the combustion zone. Another important factor is that uniform combustion over the fuel surface weakened the effect of the resulting ash barrier during the release of volatiles from the deep layers of the fuel sample, i.e., the ash crust on the particle surface clogged some of its porous channels and did not allow the release of all the volatiles for the gas-phase burnout. The coke formation on the particle surface slightly suppressed the heterogeneous combustion of carbon.

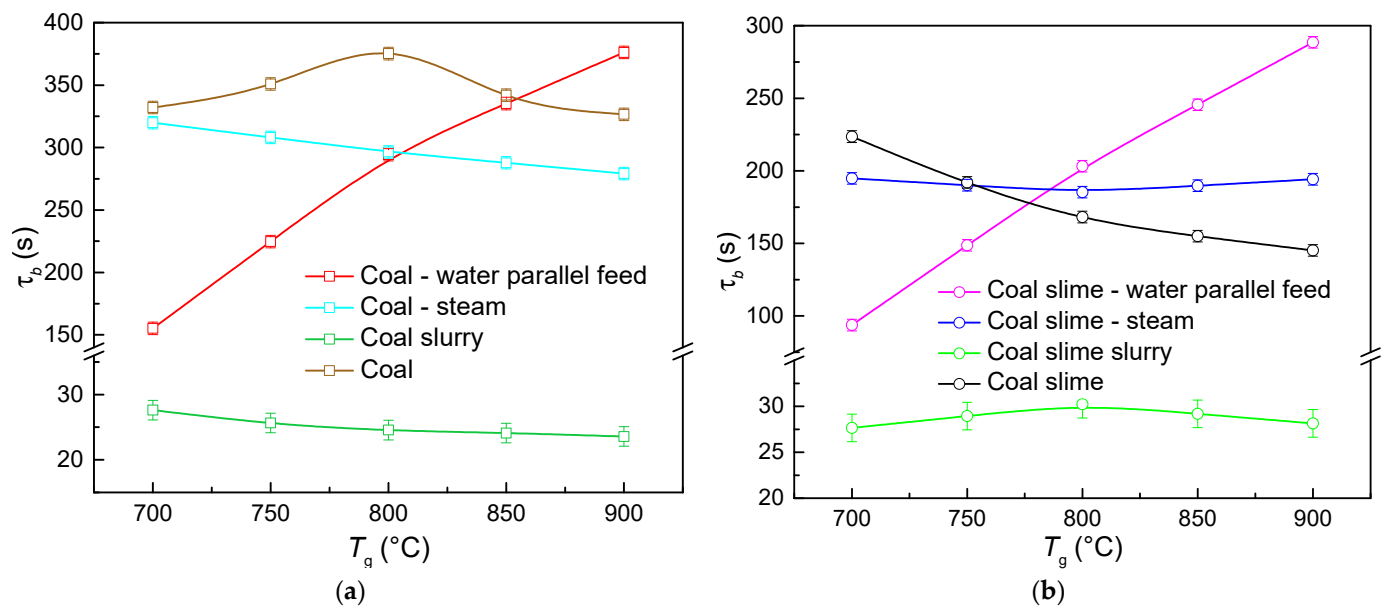


Figure 8. Combustion duration of fuels based on bituminous coal (a) and coal slime (b) when varying the method of introducing the components and temperature in the combustion chamber.

The comparison of the two types of coal components reveals that the combustion duration of coal samples (except for slurry droplets) is higher than that of coal slime. This result is related to the fuel characteristics. Coal slime is a high-ash waste with quite a low content of combustible mass. Consequently, it takes less time for it to burn out completely. It is possible to assume that the steam-air environment intensified the interaction of the oxidizer with the coke residue of the slime, thus leading to the growth of its combustion rate. At temperatures exceeding $750\text{ }^{\circ}\text{C}$ in the combustion chamber, the duration of coal slime combustion in the steam environment increased by 9–25% compared to the same characteristics of the reaction of slime particles in the air. The steam intensified the diffusion transfer of oxygen to the inner layers of the fuel. During coal slime combustion at high temperatures, it slowed down due to the gradual formation of a dense ash envelope. A similar finding was obtained in the study [26], which analyzed the effect of steam on the combustion characteristics of pulverized coal using a thermogravimetric analyzer during oxy-fuel combustion. A decrease in the burnout time and an increase in the mass-loss rate (by up to 35%) were observed after steam was added to the combustion atmosphere.

Figure 9 presents the curves of the relative indicator of the fuel burnout versus the temperature in the combustion chamber, given by:

$$m = (m_0 - m_1) / m_0 \cdot 100\%, \quad (2)$$

where m_0 is the initial sample mass, and m_1 is the mass of the unburnt char.

In line with Equation (1), the greater the value of m , the more complete the fuel burnout. The obtained relative indicators of burnout (Figure 9) are quite consistent with the data on the effects of the temperature in the furnace on the fuel combustion time (Figure 8). The experiments showed that, with the parallel supply of coal and water, the mass-loss rate (Figure 9a) was lower compared to direct steam injection. At lower temperatures, the combustion of coal with nearby water droplets stopped before the entire combustible part of the fuel had time to react (due to the loss of energy for the evaporation of water). So, at a temperature of $700\text{ }^{\circ}\text{C}$, the mass of the unburned part (m_1) was commensurate with the mass remaining during the combustion of coal in air. The increase in temperature intensified the burnout of coal with the parallel supply of the components. The direct steam supply was characterized by higher values of the relative burnout index, which ranged from 81 to 88%. This result indicates an intensification of oxidant diffusion and carbon gasification in the vapor environment, which improved fuel burnout.

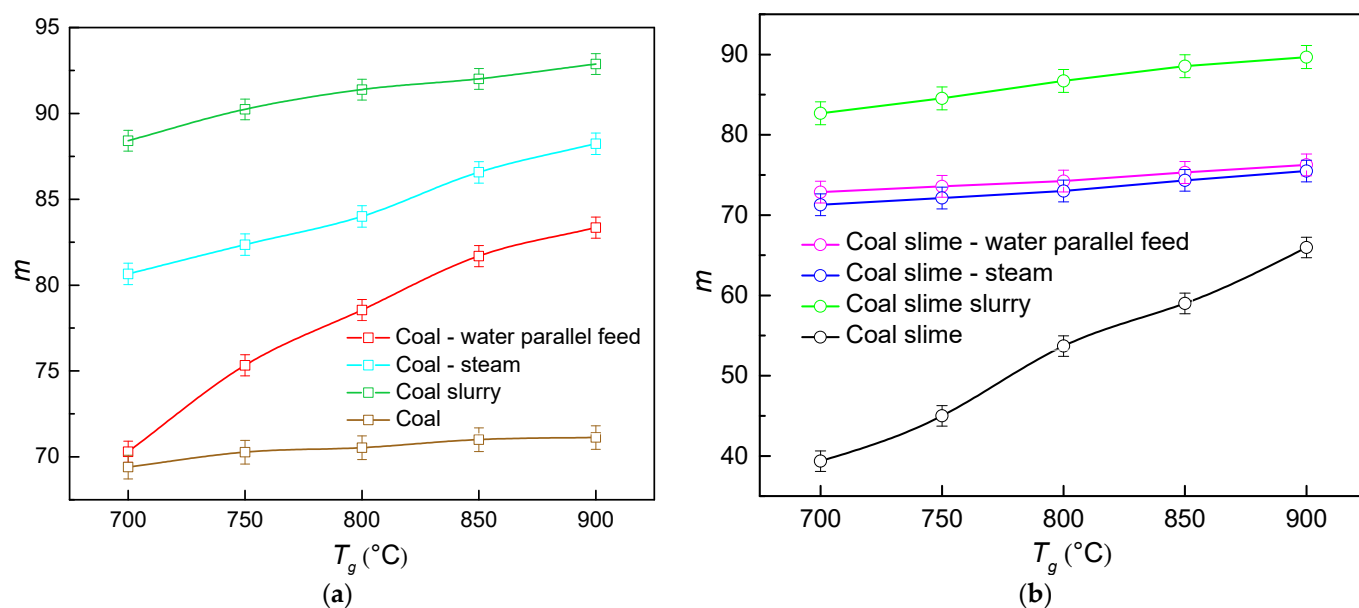


Figure 9. Relative indicator of completeness of reactions of fuels based on bituminous coal (a) and coal slime (b) when varying the scheme of introducing the components and temperature into the combustion chamber.

When burning coal slime (Figure 9b), no noticeable differences in the burnout characteristics were recorded when water and slime were supplied separately, or when steam was used. The difference between the corresponding coefficients did not exceed 2%. The characteristics of the coal slime, in particular the high ash content and the presence of floculants, had a greater effect on the burnout rate. Although steam intensified the diffusion transfer of oxygen to the inner layers of the fuel, at high temperatures this process slowed down due to the gradual agglomeration of ash particles in the pores.

The maximum burnout rate was recorded during the reactions of slurry fuels based on coal slime and bituminous coal. As with the combustion duration, this effect is conditioned by the even heating and burnout of fuel droplets. Compared with coal and coal slime reacting in the air, the burnout indicator of slurry fuels increased by 21–23 and 26–52%, respectively. In general, the comparison of the two coal components indicates that the burnout indicator of coal is up to 15% higher than that of coal slime due to the high ash content of the latter (Table 1). One important finding is that the formation of a steam-air environment due to the evaporation of nearby water droplets or steam injection makes it possible to increase the degree of carbon burnout by up to 46%. This effect is more pronounced for coal slime (especially in the low-temperature range).

Table 2 presents the experimental research findings for the effect of steam content on the temporal characteristics of the ignition and combustion of coal powder at a temperature of 800 °C in the combustion chamber. An increase in the steam content was shown to lead to higher delay times of gas-phase and heterogeneous ignition. It took more time to heat the created steam-air environment. However, the opposite effect is produced by an increase in the steam content throughout the duration of coal combustion. The duration of the sample combustion decreased by 10% with a twofold increase in the steam content. The result is attributed to the fact that the steam-air environment intensified the interaction of the oxidizer with the coke residue and enhanced the heat transfer to the deep fuel layers.

Table 2. Effect of steam content on the temporal characteristics of combustion.

Steam/Coal Ratio	τ_{d1} , s	τ_{d2} , s	τ_b , s
1/2	2.95	17.78	314.73
1/1	3.20	18.29	296.43
2/1	3.48	18.88	284.14

4.4. Environmental Characteristics of Combustion

Figure 10 presents the curves of the average concentrations of carbon dioxide plotted for the examined schemes of fuel combustion. The comparison of CO₂ concentrations released from the combustion of coal and coal slime in the air revealed that using water (as a separate component, steam or in the slurry composition) makes it possible to reduce CO₂ emissions from 20 to 61%. This effect is accounted for by a decrease in the temperature in the combustion zone. Compared with slurries, the steam contributed to higher concentrations of carbon dioxide. The presence of steam increased the duration of the gas-phase combustion with a proceeding reaction [35–37]:

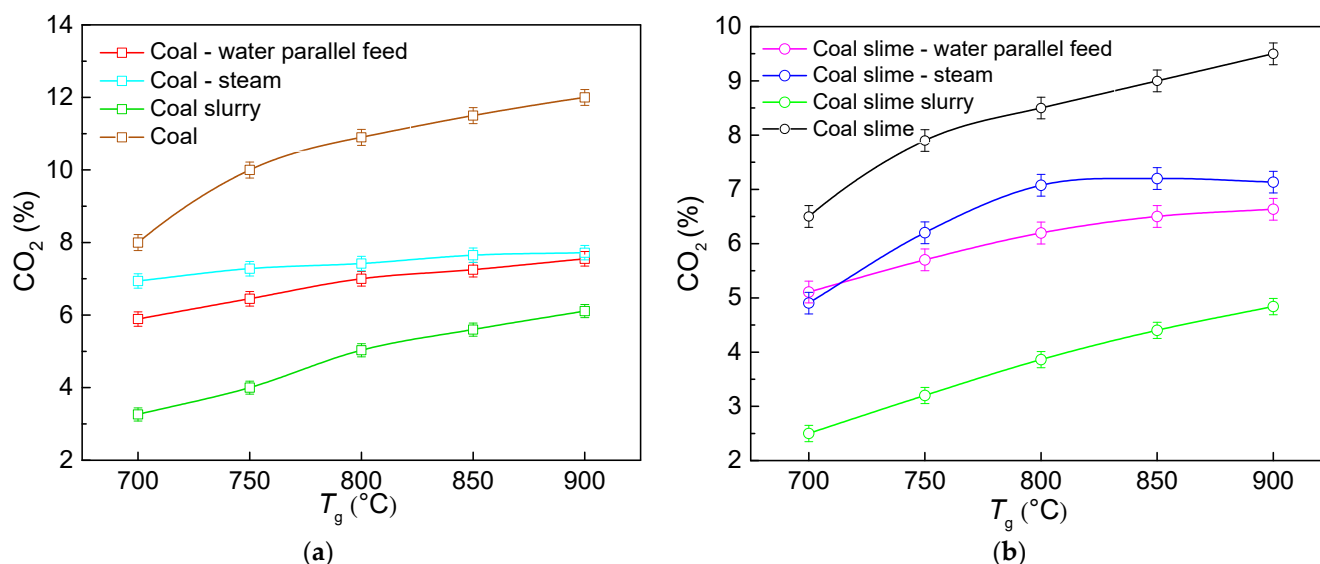


Figure 10. Average concentrations of carbon dioxide when varying the method of introducing the coal component (coal (a) and coal slime (b)) and water, as well as the temperature in the combustion chamber.

The subsequent oxidation of hydrogen resulted in OH hydroxyl, H and O atoms. The presence of active hydroxyl centers and atomic hydrogen in the flame zone intensified the reactions of oxidation and combustion of the hydrocarbon fuel. Additional trajectories of hydroxyl radical formation are given by [38]



The reactions (4) and (5) proceed in a rather wide temperature range from 20 to 2200 °C [39], yet with a temperature increase, the constants of the rates of these reactions significantly increase. Thus, with the temperature increasing from 500 to 700 °C, the rate constants increased up to 12 times, and with an increase from 700 to 900 °C, by up to 5.5 times. This indicates that, in the temperature range under consideration, the reactions are expected to proceed steadily [39].

Thus, the catalytic effect of steam on the combustion of carbon monoxide (CO) is related to the reaction (6), resulting in an increase in the carbon dioxide concentrations [39]:



Like the reactions (4) and (5), the reaction (6) proceeds in the temperature range from 20 to 2200 °C [39], yet at 700 °C, the rate constant changed by no more than 10% with a temperature rise by every 100 °C (in the temperature range from 20 to 600 °C, the difference in the rate constants when varying the temperature by 100 °C was 12–16%) [39]. Moreover, a temperature rise increased the fuel combustion rate and intensified the release of volatiles from the fuel, which led to lower oxygen concentrations near the surface of the burning particles. Thus, the CO concentrations in the flame front increased (reaction R1). As a result, the interaction of steam with carbon (reaction (1)) and CO (reaction (3)) intensified towards the formation of CO₂.

The analysis of the results (Figure 11) suggests that introducing water into the combustion chamber significantly reduces the NO emissions (by up to 2.7 times). This effect became especially noticeable at temperatures above 800 °C. The evaporation of water with a relatively high molar heat capacity and absorbing heat and the low partial pressure of oxygen produce a combined effect. This reduces the combustion temperature and hence slows down the formation of nitrogen oxides. The plotted curves are consistent with the research findings in [22], which studied the combustion and pollutants of water-emulsified fuel. An increase in water content was shown [22] to reduce the NO_x concentrations by up to 70%. The latter was explained by a temperature decrease (of up to 17%) in the combustion chamber, in particular, due to a reduction in the peak flame temperature during combustion. Moreover, it was assumed that the presence of water increased the amount of OH radicals that reacted with excess oxygen and caused the reduction of NO_x [22].

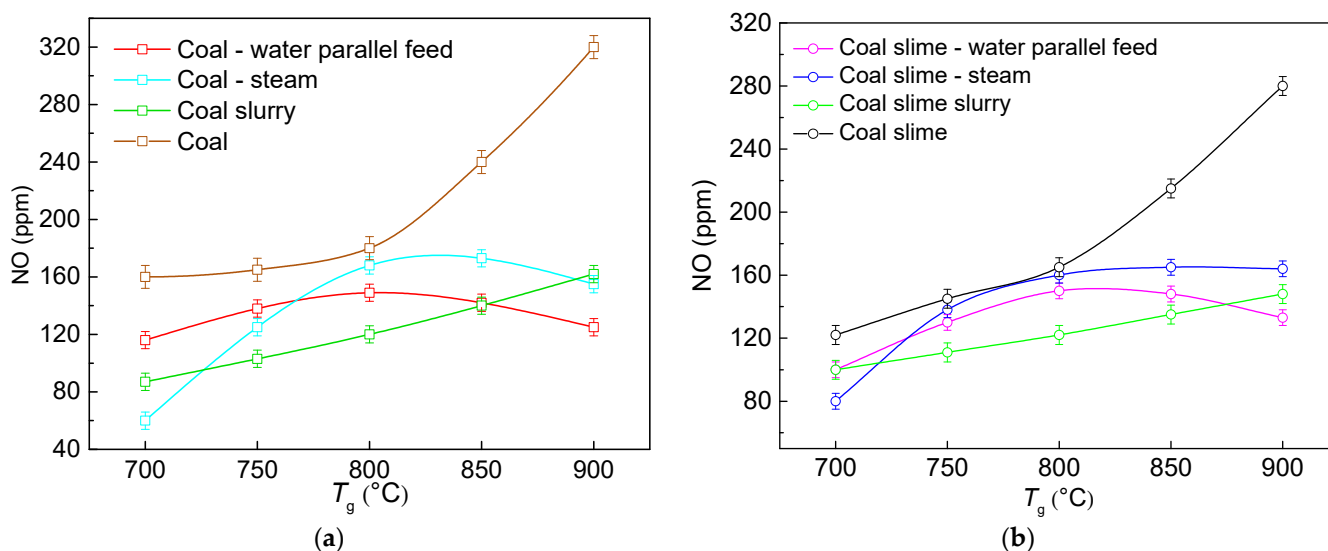


Figure 11. Average concentrations of nitrogen oxide when varying the method of introducing the coal component (coal (a) and coal slime (b)) and water, as well as the temperature in the combustion chamber.

The shapes of the curves of nitrogen oxide concentrations versus the temperature in the chamber with the simultaneous introduction of water, in the form of steam, and the coal component were rather surprising (Figure 11). In the temperature range from 700 to 800 °C, the concentrations increased and reached peak values at 800 °C. A further increase in the temperature to 900 °C was characterized by a steady decrease in NO concentrations to values close to those for the slurry combustion. It was established that the creation of a steam environment during the combustion of coal fuel intensified the release of volatiles

and increased the reactivity of the fuel due to the heat released from their combustion. Moreover, the gasification of char with steam increased the porosity of its particles, thus contributing to the diffusion of oxygen into the deep fuel layers. This resulted in a higher burnout degree and a greater amount of nitrogen reacting in the combustion, which caused NO to increase [40] in the temperate range between 700 and 800 °C. Similar effects were discussed in [20]. Wang et al. [20] investigated the effect of a steam environment on the characteristics of the isothermal combustion of coal in a thermogravimetric experimental system. The content of the steam varied, in the range of 10–30%. Wang et al. [20] established that, with an increase in the steam concentration, the TG curves shifted towards lower times, which indicated an increased mass-loss rate of char and a decreased burnout time. The authors explained this result by the fact that the gasification of coal with steam could occur at a low oxygen concentration, which increased the porosity of coal particles.

However, at a higher temperature (900 °C), the steam molecules could react with coal particles and CO to produce active hydrogen (H) atoms and active hydroxyl (OH) radicals which participated in the reactions of NO reduction with the help of NH₃ [41,42]:



For the reactions (7)–(9), at temperatures above 900 °C, constants reach certain values, and with a temperature increase of 100 °C, the difference between the constants does not exceed 10% [39,43,44]. This suggests that at temperatures above 900 °C, the above reactions can proceed sustainably.

It was established that in the temperature range of 725–850 °C, the lowest concentrations of nitrogen oxides were recorded during the combustion of slurry droplets. For all the schemes of introducing coal component samples and water into the combustion chamber, the shapes of the curves obtained during the combustion of coal and coal slime correlate favorably with each other. The difference in nitrogen oxide concentrations was recorded. In general, they were 20% higher for coal than for coal slime. This effect is explained by the different content of fuel nitrogen (Table 1) which is 5% higher for coal (accounting for the ash content of the components) [41]. As the ash content of coal slime is up to 1.5 times as high, the combustible part of the fuel (made up primarily of the fuel nitrogen) is lower. As a result, NO concentrations in the decomposition and oxidation stage during coal slime combustion are lower.

According to the data obtained (Figure 12), the concentrations of sulfur oxides decreased by 30–75% when water was used in the combustion of dry coal fuels in the air. The minimum SO₂ emissions corresponded to the combustion of slurries within the whole temperature range. The difference in the concentrations between the slurries and dry coal components (coal/slime) burned in a steam-air environment varied in the range of 8–60%. This result is conditioned by the specific aspects of the gas-phase combustion of coal slime and coal. The creation of a steam-air environment contributed to the energy accumulation near the heated layer of coal particles, which activated the release of volatiles and led to the active oxidation of sulfur-containing components.

Figure 13 shows the trends (as illustrated by coal slime) constructed for the concentrations of sulfur oxides when varying the method of fuel combustion. At the stage of the release of volatile substances (gas-phase combustion, time interval 50–150 s), sulfur oxide concentrations were maximum and then they decreased. These amplitudes were minimum during the combustion of coal slime in the slurry composition. The presence of steam, on the contrary, intensified the formation of sulfur oxides at the stage of the release of volatile particles. The peak concentrations of SO₂ from the fuel combustion in a steam-air environment increased up to sevenfold relative to the slurry combustion. At the stage of heterogeneous combustion (time interval 200–700 s), the concentrations of sulfur oxides when steam was injected were higher than during the parallel introduction

of the components, which increased the average concentrations (Figure 10b). However, the duration of gas release when steam was injected decreased compared to the scheme in which water droplets were located near the coal sample on a substrate.

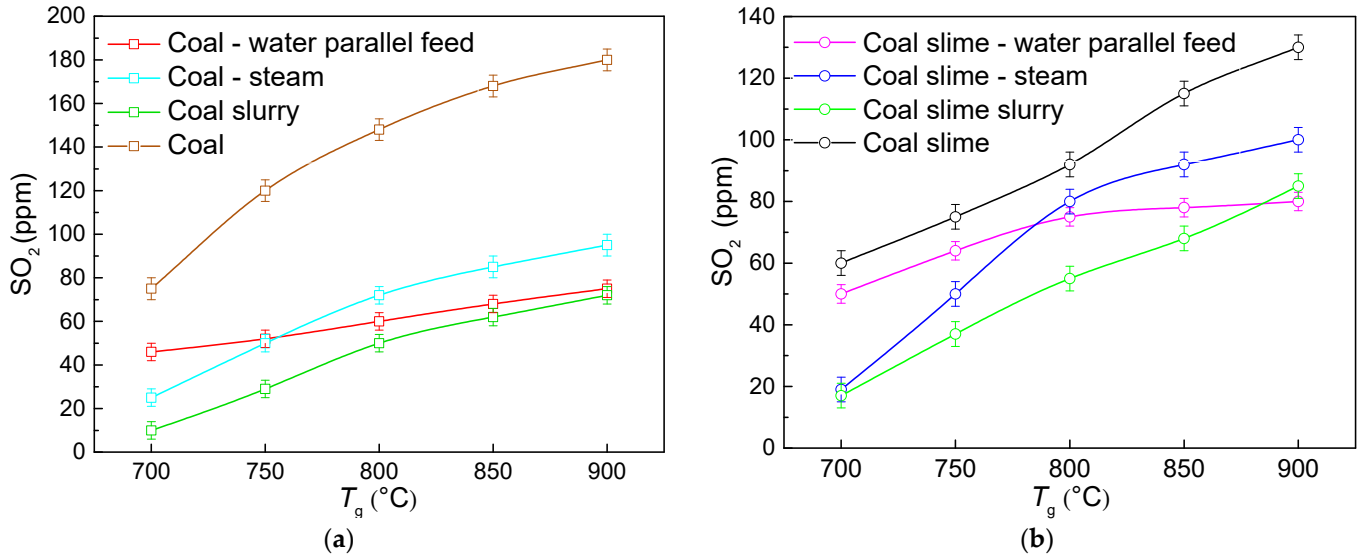


Figure 12. Average concentrations of sulfur oxide when varying the method of introducing the coal component (coal (a) and coal slime (b)) and water, as well as the temperature in the combustion chamber.

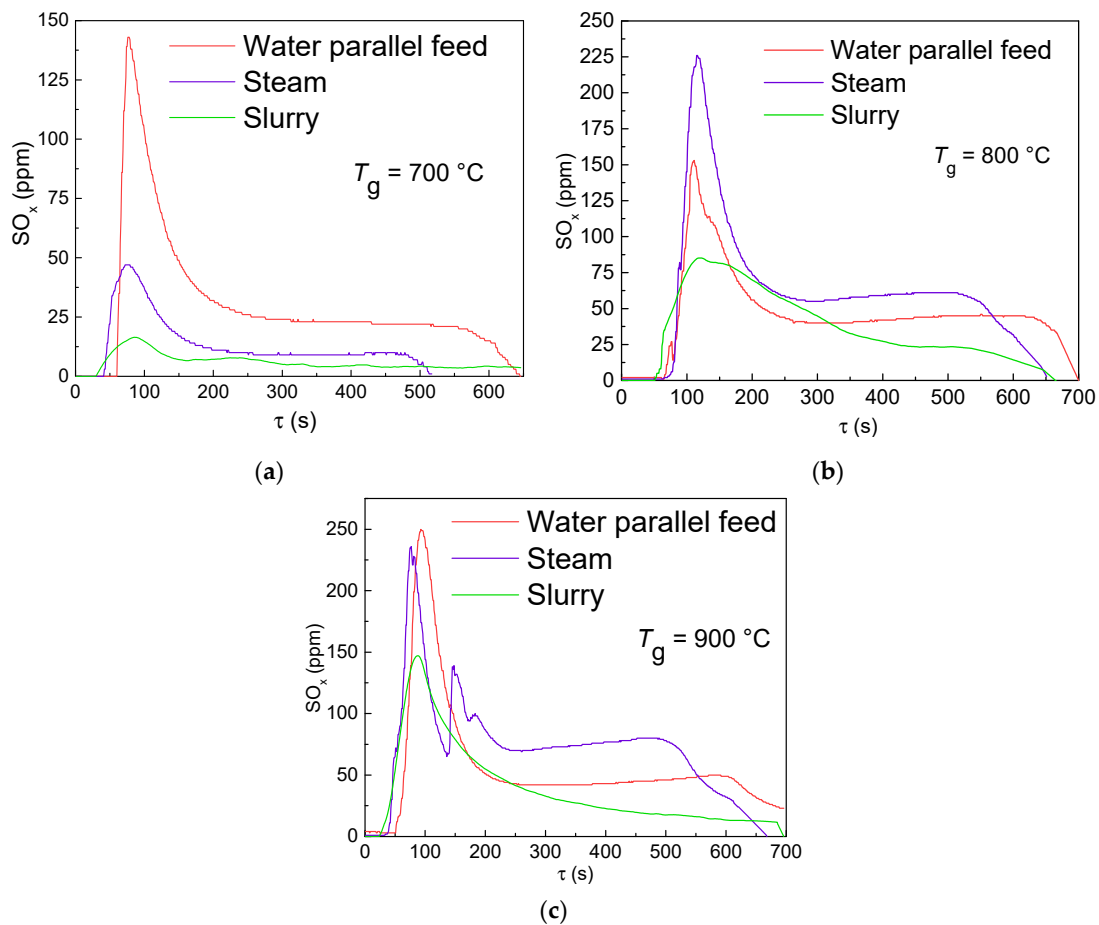


Figure 13. Trends of sulfur oxide concentrations when varying the method of coal slime and water introduction and temperature in the combustion chamber: (a) 700 °C; (b) 800 °C; (c) 900 °C.

4.5. Relative Efficiency Indicators of Fuel Combustion

To determine the most efficient fuel, the relative efficiency indicators were calculated, controlling for the obtained energy and environmental characteristics. The weighted sum method (WSM) consisting of several stages was applied [45]. The best value in each of the recorded parameters was chosen. Then the values were normalized relative to the best value. The best value for the gas-phase and heterogeneous ignition delay, ignition temperature and the concentration of anthropogenic emissions was the minimum one in a series. For the burnout coefficient and maximum combustion temperature, the maximum value in a series was chosen as optimal. At the final stage, relative efficiency indicators were given by:

$$A_n = \sum y_j \cdot X_{ij} \tag{10}$$

where y_j is the weight for each criterion, and X_{ij} is the normalized value of a criterion.

All the weight coefficients totaled 1. In this research, all the weight coefficients were assumed equal. Using this approach, the best fuel is the one whose efficiency indicator (A_n) is maximum. The calculation results are presented in Figure 14. It is shown how the complex efficiency indicator changes for the three considered methods for the combustion of coal components and water when varying the temperature in the combustion chamber. Within the whole range of temperatures in the furnace, the obtained coefficients for the slurry exceeded those for the fuels burned in the steam or air environment by 7–35% and 34–47%, respectively. This result shows great prospects of burning fuel slurries, especially those based on coal slime, because it is possible to significantly reduce the gas-phase and heterogeneous ignition delay times, minimum ignition temperature, concentrations of anthropogenic gases and losses due to incomplete burnout.

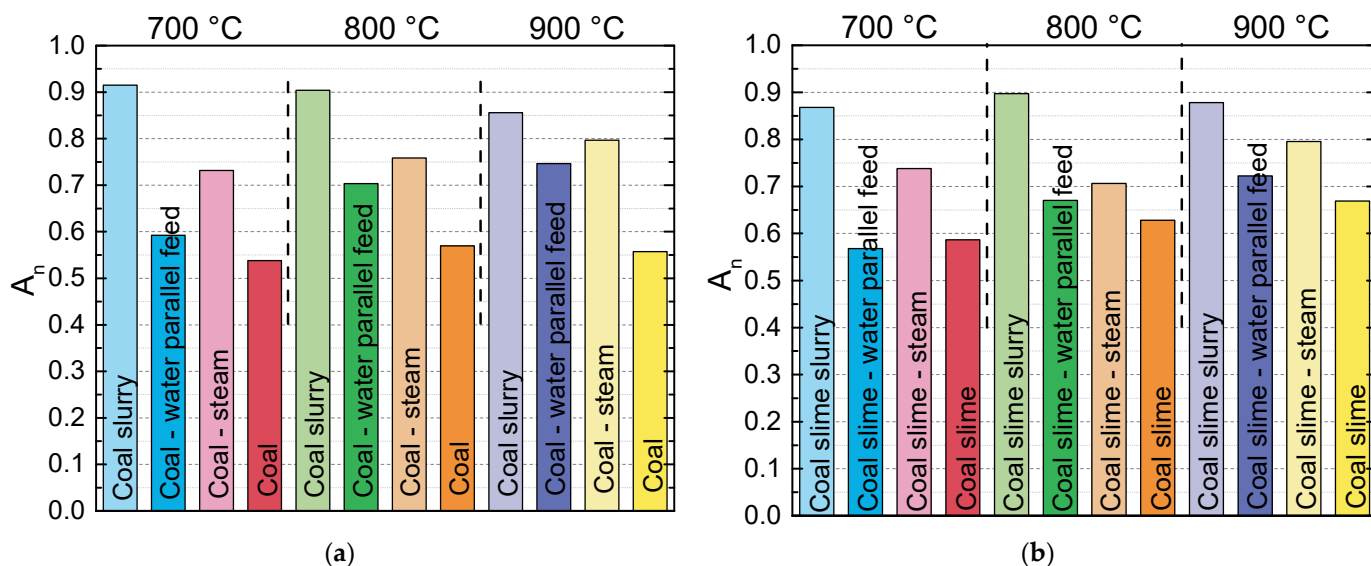


Figure 14. Efficiency indicators of fuels based on coal (a) and coal slime (b).

To illustrate the contribution of each component to the A_n coefficient, a vector diagram for the fuels based on coal slime is presented in Figure 14, as the comparison of two coal components at 800 °C and 900 °C (Figure 15) showed that slime-based slurries have the highest efficiency indicators. According to the data obtained (Figure 15), six out of eight of the relative indicators under consideration for the slurry are maximum. The surface area for the slurry in the vector diagram is larger than for the two other examined methods for the combustion of slime and water. The biggest contribution to the above increase comes from the indicators of heterogeneous ignition, burnout and carbon dioxide emissions.

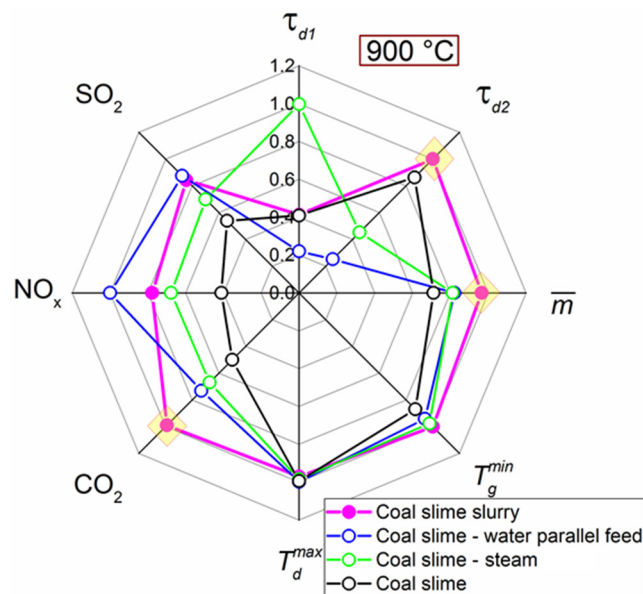


Figure 15. Efficiency indicators of the examined methods of coal slime combustion with water (at a temperature of 900 °C in the combustion chamber).

However, potentially negative aspects of slurry use are a decrease in available heat due to a lower calorific value. Therefore, it is advisable to carry out initial assessments of the boiler heat balance and changes in the efficiency coefficient when burning slurry or supplying steam. The parallel supply of water and the coal component is not considered in the calculation, since this method was characterized by lower values of the efficiency indicators (Figure 14), in comparison with steam and slurry.

The heat balance of the boiler is determined by Equation (11):

$$Q = Q_1 + Q_2 + Q_3 + Q_4 + Q_5 + Q_6, \quad (11)$$

where Q —the available heat of the fired coal; Q_1 —heat usefully used in the boiler; Q_2 —heat loss through stack gas; Q_3 —heat loss by chemical unburned fuel; Q_4 —heat loss owing to mechanical unburned fuel; Q_5 —heat loss from external cooling; and Q_6 —heat loss through the sensible heat of ash and slag.

To express the heat losses in percentages, we divide both sides by the Q :

$$100\% = q_1 + q_2 + q_3 + q_4 + q_5 + q_6, \quad (12)$$

The efficiency of the boiler can be assessed through the calculation of the efficiency coefficient. Boiler efficiency is defined by the ration of heat absorbed by the boiler and the heat provided by the fuel:

$$\eta = q_1 = 100 - (q_2 + q_3 + q_4 + q_5 + q_6). \quad (13)$$

Available heat of the fired coal.

The total heat input to the fired coal is given by:

$$Q = LHV + H_f + Q_{wr} + Q_{wh} + Q_{cd} \quad (14)$$

where, LHV—lower heating value; H_f —the sensible heat of the fuel; Q_{wr} —sensible heat carried by the air when heated by the external air heater; Q_{wh} —the heat of the fuel atomizing steam; and Q_{cd} —heat spent in the decomposition of carbonates.

The sensible heat of fuel (only for liquid and gaseous fuels) is given by:

$$H_f = c_{pf} \cdot T_f \quad (15)$$

where c_{pf} —specific heat of the fuel as received, and T_f —fuel temperature at the burner.

The heat carried by the air is determined only when it is preheated in a heater. In this calculation, we assume that $Q_{wr} = 0$ MJ/kg.

The heat of the fuel-atomizing steam is given by

$$Q_{wh} = G_s \cdot (h_s - h_{fg}), \quad (16)$$

where G_s —specific steam consumption required for atomization of 1 kg of fuel; h_s —enthalpy of steam for blowing (at an absolute pressure of saturated steam $h_s = 2.79$ MJ/kg); and h_{fg} —steam enthalpy contained in flue gases (conditionally taken equal to 2.5 MJ/kg).

The heat of the fuel atomizing steam during the dry coal combustion and slurry was assumed to be zero.

The heat spent in the decomposition of carbonates is taken into account only in cases of oil shale combustion. In this calculation, it is equal to zero.

Heat losses

The heat lost to flue gases is given by:

$$q_2 = ((h_{fg} - \alpha_{ah} h_a^0) \cdot (100 - q_4)) / Q \quad (17)$$

where h_{fg} —flue gas enthalpy; h_a^0 —theoretical cold air enthalpy entering the boiler; and α_{ah} —excess air coefficient of flue gases.

The flue gas enthalpy is determined from the reference data and depends on the flue gas temperature. Taking into account the fact that the normalized moisture content of dry coal and slime is $W_n < 0.7\% \cdot \text{kg/MJ}$, and that of slurry is $1 < W_n < 5\% \cdot \text{kg/MJ}$, we accept the flue gas temperatures as 120 and 130 °C, respectively. Consequently, flue gas enthalpy for dry and wet fuels was 2.89 and 1.86 MJ/kg, respectively.

The heat loss owing to mechanical unburned fuel is determined according to reference data, taking into account the fuel type and combustion device. According to the data of [46], during the combustion of coal waste with a normalized ash content $A_n \geq 1.4$ kg/MJ, the value of q_4 is assumed to be 4%. During the combustion of coking coal, q_4 was taken to be equal to 8%. The losses with physical underburning during the combustion of slurry fuels decrease relative to coal and sludge, since CWS drops intensively fragment directly in the combustion chamber. For slurry, q_4 was taken to be equal to 2%.

The chemical incomplete combustion loss q_3 is generally small. For example, for a pulverized coal furnace, q_3 should be no more than 0.5%. During the combustion of CWS, the proportion of non-oxidized fuel is less. Water vapor formed during the injection of the fuel composition in the combustion chamber intensifies the oxidative processes. A similar process occurs with steam injection. Therefore, it was assumed that q_3 for suspensions and steam injection was 0.2%.

Heat losses from external cooling q_5 are determined from empirical data depending on the boiler steam output [46]. At the nominal steam capacity of the boiler $D = 10$ t/h, the heat loss from external cooling is 1.85%.

The heat loss through the sensible heat of ash and slag q_6 can be determined by the formula:

$$q_6 = (100 - \alpha_{ash}) \cdot h_{ash} \cdot A^r / Q \quad (18)$$

where α_{ash} —fly ash fraction; h_{ash} —ash enthalpy; and A^r —ash content of fuel per operating weight.

Based on the above methodology, the calculation of the heat balance of the boiler unit was carried out. Parameter values and calculation results are presented in Table 3.

According to the Table 3 estimates, it was found that the maximum boiler efficiency is achieved by slurry combustion. The value of η increased by 3.5–8% in comparison with the combustion of dry pulverized coal. Steam injection also led to an increase in efficiency, but the difference did not exceed 0.4%.

Table 3. Calculation results of boiler heat balance.

Parameter	Schemes of Fuel Combustion					
	Coal	Coal Slurry	Coal–Steam	Coal Slime	Coal Slime Slurry	Coal Slime–Steam
LHV, MJ/kg	28.7	13.8	28.7	23.6	11.2	23.6
c_{pf} , kJ/kg·°C	1.05	2.62	1.05	1.89	3.05	2.05
T_f , °C	0	80	0	0	80	0
G_s , kg/kg	–	–	0.1	–	–	0.1
h_s , kJ/kg	–	–	2.79	–	–	2.79
h_{fg} , kJ/kg	2.5	2.5	2.5	2.5	2.5	2.5
α_{ah}	1.58	1.58	1.58	1.58	1.58	1.58
h_a^0 , kJ/kg	1.005	0.256	1.005	1.005	0.256	1.005
α_{ash}	0.15	0.15	0.15	0.5	0.5	0.5
h_{ash} , kJ/kg	0.56	0.56	0.56	0.56	0.56	0.56
A^r , %	14.65	7.32	14.65	26.46	13.23	26.46
Q , MJ/kg	28.70	14.03	28.73	23.61	11.44	23.64
H_f , MJ/kg	0	0.21	0	0	0.24	0
Q_{wh} , MJ/kg	0	0	0.03	0	0	0.03
q_2 , %	2.92	9.74	2.91	3.75	10.27	3.74
q_3 , %	0.5	0.2	0.2	0.5	0.2	0.2
q_4 , %	8	2	8	4	2	4
q_5 , %	1.85	1.85	1.85	1.85	1.85	1.85
q_6 , %	0.29	0.29	0.28	0.62	0.64	0.62
η , %	82.65	89.29	82.97	84.50	87.49	84.82

The experimental results contribute to the optimization of the fuel and steam-air medium supply modes (using separate nozzles or devices for the simultaneous supply of fuel and steam) to increase the efficiency of fuel combustion and minimize emissions. The results obtained can be used in technologies for preparing fuel for combustion by its fine and uniform atomization, as well as mixing with an oxidizing agent. This direction is applicable in the design of nozzles and burner devices. In practice, the use of water in the composition of fuel slurries or the creation of a vapor-air medium in the combustion chamber will solve several significant problems such as reducing heat loads, preventing detonations in combustion chambers, and intensifying the micro-explosive dispersion of slurry. The creation of a finely dispersed gas-droplet flow, which ensures the efficient mixing of combustible components and oxidizers, in turn, prevents the clogging and coking of nozzles and burners.

5. Conclusions

- (i) The creation of a steam-air atmosphere in the combustion chamber significantly affects the ignition and combustion characteristics of coal fuels, including those with low reactivity. The steam injection led to a reduction in the gas-phase ignition delay time by 5–50% compared to the simultaneous introduction of water and coal components or when using a coal–water slurry. Moreover, when steam was supplied, the heterogeneous ignition times of the coke residue were reduced by 46–52% in comparison with coal dust combustion. It is also shown that the steam-air environment allows for an increase in the burnout degree of coal fuel samples by 46%.
- (ii) At the same time, slurry fuels based on coal and coal slime were characterized by the shortest burning times. The difference between slurry and dry coal components was 80–93%. Additionally, it was established that using water in the slurry composition is the most environmentally promising method. The average concentrations of CO₂, NO and SO₂ decreased by 19–53%, 9–28% and 30–78%, respectively, relative to when water was introduced separately on a substrate and as steam.
- (iii) The calculated values of complex efficiency indicators showed that the most preferable scheme for burning coal fuels is to turn them into water-containing slurries. The

cumulative indicator is 7–47% higher for slurries than for the other options under consideration. The research provides substantial evidence for developing the combustion technologies of sprayed fuel slurries based on coal and coal slime.

Supplementary Materials: The following supporting information can be downloaded at: <https://www.mdpi.com/article/10.3390/en15249591/s1>, Video S1: Video demonstrating the combustion of fuels.

Author Contributions: Methodology, investigation, visualization, V.D.; data curation, writing-review and editing, G.K.; methodology, formal analysis, investigation, visualization, writing-original draft, writing-review and editing, G.N. All authors have read and agreed to the published version of the manuscript.

Funding: The authors are grateful for the financial support received from the Tomsk Polytechnic University (TPU) development program Priority 2030 (Priority-2030-NIP/EB-038-1308-2022).

Data Availability Statement: Not applicable.

Conflicts of Interest: The authors declare no conflict of interest.

References

1. Fraga, L.G.; Silva, J.; Teixeira, J.C.; Ferreira, M.E.C.; Teixeira, S.F.; Vilarinho, C.; Gonçalves, M.M. Study of Mass Loss and Elemental Analysis of Pine Wood Pellets in a Small-Scale Reactor. *Energies* **2022**, *15*, 5253. [\[CrossRef\]](#)
2. *International Energy Agency Key World Energy Statistics*; IEA: Paris, France, 2020; p. 80.
3. Askarova, A.; Zamorano, M.; Martín-Pascual, J.; Nugymanova, A.; Bolegenova, S. A Review of the Energy Potential of Residual Biomass for Coincineration in Kazakhstan. *Energies* **2022**, *15*, 6482. [\[CrossRef\]](#)
4. Arslan, O.; Erbas, O. Investigation on the Improvement of the Combustion Process through Hybrid Dewatering and Air Pre-Heating Process: A Case Study for a 150 MW Coal-Fired Boiler. *J. Taiwan Inst. Chem. Eng.* **2021**, *121*, 229–240. [\[CrossRef\]](#)
5. Deng, L.; Zhao, Y.; Sun, S.; Feng, D.; Zhang, W. Review on Thermal Conversion Characteristics of Coal in O₂/H₂O Atmosphere. *Fuel Process. Technol.* **2022**, *232*, 107266. [\[CrossRef\]](#)
6. Qiu, S.; Reddy, R.G.; Huang, X.; Yin, C.; Zhang, S. Relationships between Combustion Behavior in Air and the Chemical Structure of Bituminous Coal during Combustion Processes. *Energies* **2022**, *15*, 5154. [\[CrossRef\]](#)
7. Munawer, M.E. Human Health and Environmental Impacts of Coal Combustion and Post-Combustion Wastes. *J. Sustain. Min.* **2018**, *17*, 87–96. [\[CrossRef\]](#)
8. Asghar, U.; Rafiq, S.; Anwar, A.; Iqbal, T.; Ahmed, A.; Jamil, F.; Khurram, M.S.; Akbar, M.M.; Farooq, A.; Shah, N.S.; et al. Review on the Progress in Emission Control Technologies for the Abatement of CO₂, SO_x and NO_x from Fuel Combustion. *J. Environ. Chem. Eng.* **2021**, *9*, 106064. [\[CrossRef\]](#)
9. Jabeen, F.; Adrees, M.; Ibrahim, M.; Mahmood, A.; Khalid, S.; Sipra, H.F.K.; Bokhari, A.; Mubashir, M.; Khoo, K.S.; Show, P.L. Trash to Energy: A Measure for the Energy Potential of Combustible Content of Domestic Solid Waste Generated from an Industrialized City of Pakistan. *J. Taiwan Inst. Chem. Eng.* **2022**, *137*, 104223. [\[CrossRef\]](#)
10. Suleimenova, B.; Aimbetov, B.; Zhakupov, D.; Shah, D.; Sarbassov, Y. Co-Firing of Refuse-Derived Fuel with Ekibastuz Coal in a Bubbling Fluidized Bed Reactor: Analysis of Emissions and Ash Characteristics. *Energies* **2022**, *15*, 5785. [\[CrossRef\]](#)
11. Gent, J.F.; Triche, E.W.; Holford, T.R.; Belanger, K.; Bracken, M.B.; Beckett, W.S.; Leaderer, B.P. Association of Low-Level Ozone and Fine Particles With Respiratory Symptoms in Children With Asthma. *JAMA* **2003**, *290*, 1859–1867. [\[CrossRef\]](#) [\[PubMed\]](#)
12. Li, D.; Liu, J.; Wang, S.; Cheng, J. Study on Coal Water Slurries Prepared from Coal Chemical Wastewater and Their Industrial Application. *Appl. Energy* **2020**, *268*, 114976. [\[CrossRef\]](#)
13. Nyashina, G.S.; Vershinina, K.Y.; Strizhak, P.A. Impact of Micro-Explosive Atomization of Fuel Droplets on Relative Performance Indicators of Their Combustion. *Fuel Process. Technol.* **2020**, *201*, 106334. [\[CrossRef\]](#)
14. Xiu, M.; Stevanovic, S.; Rahman, M.M.; Pourkhesalian, A.M.; Morawska, L.; Thai, P.K. Emissions of Particulate Matter, Carbon Monoxide and Nitrogen Oxides from the Residential Burning of Waste Paper Briquettes and Other Fuels. *Environ. Res.* **2018**, *167*, 536–543. [\[CrossRef\]](#)
15. Jianzhong, L.; Ruikun, W.; Jianfei, X.; Junhu, Z.; Kefa, C. Pilot-Scale Investigation on Slurrying, Combustion, and Slagging Characteristics of Coal Slurry Fuel Prepared Using Industrial Wasteliquid. *Appl. Energy* **2014**, *115*, 309–319. [\[CrossRef\]](#)
16. Dorokhov, V.V.; Kuznetsov, G.V.; Nyashina, G.S.; Strizhak, P.A. Composition of a Gas and Ash Mixture Formed during the Pyrolysis and Combustion of Coal-Water Slurries Containing Petrochemicals. *Environ. Pollut.* **2021**, *285*, 117390. [\[CrossRef\]](#) [\[PubMed\]](#)
17. Ma, X.W.; Li, F.H.; Ma, M.J.; Fang, Y.T. Fusion Characteristics of Blended Ash from Changzhi Coal and Biomass. *Ranliao Huaxue Xuebao/J. Fuel Chem. Technol.* **2018**, *46*, 129–137. [\[CrossRef\]](#)
18. Chen, L.Y.; Chen, Y.H.; Hung, Y.S.; Chiang, T.H.; Tsai, C.H. Fuel Properties and Combustion Characteristics of Jatropa Oil Biodiesel–Diesel Blends. *J. Taiwan Inst. Chem. Eng.* **2013**, *44*, 214–220. [\[CrossRef\]](#)

19. Miccio, F.; Raganati, F.; Ammendola, P.; Okasha, F.; Miccio, M. Fluidized Bed Combustion and Gasification of Fossil and Renewable Slurry Fuels. *Energies* **2021**, *14*, 7766. [CrossRef]
20. Wang, C.; Shao, H.; Lei, M.; Wu, Y.; Jia, L. Effect of the Coupling Action between Volatiles, Char and Steam on Isothermal Combustion of Coal Char. *Appl. Therm. Eng.* **2016**, *93*, 438–445. [CrossRef]
21. Yi, B.; Zhang, L.; Huang, F.; Mao, Z.; Zheng, C. Effect of H₂O on the Combustion Characteristics of Pulverized Coal in O₂/CO₂ Atmosphere. *Appl. Energy* **2014**, *132*, 349–357. [CrossRef]
22. De Giorgi, M.G.; Fontanarosa, D.; Ficarella, A.; Pescini, E. Effects on Performance, Combustion and Pollutants of Water Emulsified Fuel in an Aeroengine Combustor. *Appl. Energy* **2020**, *260*, 114263. [CrossRef]
23. Lei, K.; Zhang, R.; Ye, B.; Cao, J.; Liu, D. Combustion of Single Particles from Sewage Sludge/Pine Sawdust and Sewage Sludge/Bituminous Coal under Oxy-Fuel Conditions with Steam Addition. *Waste Manag.* **2020**, *101*, 1–8. [CrossRef]
24. Lei, K.; Ye, B.; Cao, J.; Zhang, R.; Liu, D. Combustion Characteristics of Single Particles from Bituminous Coal and Pine Sawdust in O₂/N₂, O₂/CO₂, and O₂/H₂O Atmospheres. *Energies* **2017**, *10*, 1695. [CrossRef]
25. Ma, L.; Chen, X.; Yu, S.; Fang, Q.; Zhang, C.; Chen, G. Effect of H₂O on the Combustion Characteristics and Interactions of Blended Coals in O₂/H₂O/CO₂ Atmosphere. *J. Energy Inst.* **2021**, *94*, 222–232. [CrossRef]
26. Gil, M.V.; Riaza, J.; Lvarez, L.A.; Pevida, C.; Pis, J.J.; Rubiera, F. A Study of Oxy-Coal Combustion with Steam Addition and Biomass Blending by Thermogravimetric Analysis. *J. Therm. Anal. Calorim.* **2012**, *109*, 49–55. [CrossRef]
27. Kozlov, A. Kinetics of Thermochemical Conversion of the Lignite Coal in Steam Flow. *Energy Procedia* **2019**, *158*, 2210–2214. [CrossRef]
28. Bueno-López, A.; García-García, A. Potassium-Containing Coal-Pellets for NO_x Reduction under Gas Mixtures of Different Composition. *Carbon N. Y.* **2004**, *42*, 1565–1574. [CrossRef]
29. Escudero, A.I.; Aznar, M.; Díez, L.I. Oxy-Steam Combustion: The Effect of Coal Rank and Steam Concentration on Combustion Characteristics. *Fuel* **2021**, *285*, 119218. [CrossRef]
30. Vershinina, K.Y.; Shlegel, N.E.; Strizhak, P.A. Relative Combustion Efficiency of Composite Fuels Based on of Wood Processing and Oil Production Wastes. *Energy* **2019**, *169*, 18–28. [CrossRef]
31. Pinchuk, V.A.; Sharabura, T.A.; Kuzmin, A.V. The Effect of Water Phase Content in Coal-Water Fuel on Regularities of the Fuel Ignition and Combustion. *Fuel Process. Technol.* **2019**, *191*, 129–137. [CrossRef]
32. Yang, Z.; Zhang, Y.; Liu, L.; Wang, X.; Zhang, Z. Environmental Investigation on Co-Combustion of Sewage Sludge and Coal Gangue: SO₂, NO_x and Trace Elements Emissions. *Waste Manag.* **2016**, *50*, 213–221. [CrossRef] [PubMed]
33. Akhmetshin, M.R.; Nyashina, G.S.; Strizhak, P.A. Normalizing Anthropogenic Gas Emissions from the Combustion of Industrial Waste as Part of Fuel Slurries. *Fuel* **2021**, *313*, 122653. [CrossRef]
34. Hong, D.; Li, Z.; Si, T.; Guo, X. A Study of the Effect of H₂O on Char Oxidation during O₂/H₂O Combustion Using Reactive Dynamic Simulation. *Fuel* **2020**, *280*, 118713. [CrossRef]
35. Speight, J.G. Gasification Reaction Kinetics for Synthetic Liquid Fuel Production. In *Gasification for Synthetic Fuel Production*; Woodhead Publishing: Sawston, UK, 2015; pp. 103–117. [CrossRef]
36. Chen, K.; Bai, C.; Zhao, Y.; Zhang, W.; Sun, S.; Feng, D.; Qin, Y. Numerical Study on the Effects of Reaction Conditions on Single-Particle Char Combustion in O₂/H₂O Atmospheres. *Fuel* **2022**, *329*, 125343. [CrossRef]
37. Halim, S.A.; Mohd, N.A.; Razali, N.A. A Comparative Assessment of Biofuel Products from Rice Husk and Oil Palm Empty Fruit Bunch Obtained from Conventional and Microwave Pyrolysis. *J. Taiwan Inst. Chem. Eng.* **2022**, *134*, 104305. [CrossRef]
38. Anufriev, I.S. Review of Water/Steam Addition in Liquid-Fuel Combustion Systems for NO_x Reduction: Waste-to-Energy Trends. *Renew. Sustain. Energy Rev.* **2021**, *138*, 110665. [CrossRef]
39. Baulch, D.L.; Pilling, M.J.; Cobos, C.J.; Cox, R.A.; Esser, C.; Frank, P.; Just, T.; Kerr, J.A.; Troe, J.; Walker, R.W.; et al. Evaluated Kinetic Data for Combustion Modelling. *J. Phys. Chem. Ref. Data* **1992**, *21*, 411. [CrossRef]
40. Ma, M.; Liang, Y.; Xu, D.; Sun, S.; Zhao, J.; Wang, S. Gas Emission Characteristics of Sewage Sludge Co-Combustion with Coal: Effect of Oxygen Atmosphere and Feedstock Mixing Ratio. *Fuel* **2022**, *322*, 124102. [CrossRef]
41. Xu, M.; Tu, Y.; Zeng, G.; Wang, Q.; Zhou, A.; Yang, W. Numerical Study of Further NO_x Emission Reduction for Coal MILD Combustion by Combining Fuel-Rich/Lean Technology. *Int. J. Energy Res.* **2019**, *43*, 8492–8508. [CrossRef]
42. Wategave, S.P.; Banapurmath, N.R.; Sawant, M.S.; Soudagar, M.E.M.; Mujtaba, M.A.; Afzal, A.; Basha, J.S.; Alazwari, M.A.; Safaei, M.R.; Elfasakhany, A.; et al. Clean Combustion and Emissions Strategy Using Reactivity Controlled Compression Ignition (RCCI) Mode Engine Powered with CNG-Karanja Biodiesel. *J. Taiwan Inst. Chem. Eng.* **2021**, *124*, 116–131. [CrossRef]
43. Liping, J.; Ruifeng, L. Comparative Study of Reaction Rate Constants for the NH₃ + H → NH₂ + H₂ Reaction with Globe Dynamics and Transition State Theories. *J. Theor. Comput. Chem.* **2009**, *8*, 1227–1233. [CrossRef]
44. Silver, J.A.; Kolb, C.E. Rate Constant for the Reaction NH₃ + OH → NH₂ + H₂O over a Wide Temperature Range. *Chem. Phys. Lett.* **1980**, *75*, 191–195. [CrossRef]
45. Vershinina, K.; Dorokhov, V.; Romanov, D.; Nyashina, G.; Kuznetsov, G. Multi-Criteria Efficiency Analysis of Using Waste-Based Fuel Mixtures in the Power Industries of China, Japan, and Russia. *Appl. Sci.* **2020**, *10*, 2460. [CrossRef]
46. Thermal Calculation of Boilers (Normative Method). S.-Pb.: NPO CKTI. 1998, 256. Available online: <https://www.c-o-k.ru/library/document/12668> (accessed on 20 November 2022).